Physics Letters B 757 (2016) 136–141

Contents lists available at ScienceDirect

Physics Letters B

www.elsevier.com/locate/physletb

SUSY effects in R_b: Revisited under current experimental constraints

Wei Su [a,*], Jin Min Yang [a,b,*]

[a] Institute of Theoretical Physics, Academia Sinica, Beijing 100190, China
[b] Department of Physics, Tohoku University, Sendai 980-8578, Japan

ARTICLE INFO

Article history:
Received 3 February 2016
Received in revised form 26 March 2016
Accepted 26 March 2016
Available online 31 March 2016
Editor: J. Hisano

Keywords:
Supersymmetry
R_b

ABSTRACT

In this note we revisit the SUSY effects in R_b under current experimental constraints including the LHC Higgs data, the B-physics measurements, the dark matter relic density and direct detection limits, as well as the precision electroweak data. We first perform a scan to figure out the currently allowed parameter space and then display the SUSY effects in R_b. We find that although the SUSY parameter space has been severely restrained by current experimental data, both the general MSSM and the natural-SUSY scenario can still alter R_b with a magnitude sizable enough to be observed at future Z-factories (ILC, CEPC, FCC-ee, Super Z-factory) which produce 10^9–10^{12} Z-bosons. To be specific, assuming a precise measurement $\delta R_b = 2.0 \times 10^{-5}$ at FCC-ee, we can probe a right-handed stop up to 530 GeV through chargino-stop loops, probe a sbottom to 850 GeV through neutralino-sbottom loops and a charged Higgs to 770 GeV through the Higgs-top quark loops for a large $\tan\beta$. The full one-loop SUSY correction to R_b can reach 1×10^{-4} in natural SUSY and 2×10^{-4} in the general MSSM.

1. Introduction

After the discovery of the 125 GeV Higgs boson [1,2], the primary task of the LHC is to hunt for new physics beyond the Standard Model (SM). Among various extensions of the SM, the low energy supersymmetry (SUSY) is the most appealing candidate[1] since it can solve the gauge hierarchy problem, naturally explain the cosmic cold dark matter and achieve the gauge coupling unification. The search for SUSY has long been performed both directly and indirectly. On the one hand, the colliders have directly searched for the sparticle productions. On the other hand, SUSY effects have been probed indirectly through precision measurements of some low energy observables.

$R_b \equiv \Gamma(Z \to \bar{b}b)/\Gamma(Z \to hadrons)$ is a famous observable which is sensitive to new physics beyond the SM [4]. So far the most precise experimental value $R_b^{\rm exp} = 0.21629 \pm 0.00066$ comes from the LEP and SLC measurements [5], while the SM prediction is $R_b^{SM} = 0.21579$ [6]. The future Z-factories are expected to produce much more Z-bosons than the LEP experiment. For example, 10^9, 10^{10} and 10^{12} Z-bosons are expected to be produced respectively at the International Linear Colldier (ILC) [7], the Circular Electron–Positron Collider (CEPC) [8], the Future Circular Collider (FCC-ee) [9] and the Super Z-factory [10]. This will allow for a more precise measurement of R_b [11] and help pin down the involved new physics effects.

The SUSY effects in R_b were calculated and discussed many years ago [12–15]. In this work we revisit these effects for two reasons: (i) The current experiments, especially the LHC experiments, have severely restrained the SUSY parameter space. It is intriguing to figure out the possible magnitude of the SUSY effects in the currently allowed parameter space; (ii) Given the possibility of some future Z-factories like ILC, CEPC or FCC-ee, a more precise measurement of R_b will help reveal the SUSY effects although these effects may have already been restrained to be rather small by current experiments. In order to know if the SUSY effects are accessible in a future measurement of R_b, we must figure out their currently allowed value.

This work is organized as follows. In Sec. 2, we give a description of SUSY effects in R_b. In Sec. 3, we scan over the SUSY parameter space and display the SUSY effects in the allowed parameter space. Finally we give our conclusion in Sec. 4.

2. SUSY corrections to R_b

Since the SUSY effects in R_b have been calculated in the literature [12,13], here we only give a brief description. The dominant SUSY effects in R_b are from the vertex corrections to $Z \to b\bar{b}$, as

* Corresponding authors.
E-mail addresses: weisv@itp.ac.cn (W. Su), jmyang@itp.ac.cn (J.M. Yang).

[1] Confronted with the 125 GeV Higgs mass, the minimal SUSY model (MSSM) has a little fine-tuning while the next-to-minimal SUSY model is more favored [3].

http://dx.doi.org/10.1016/j.physletb.2016.03.075

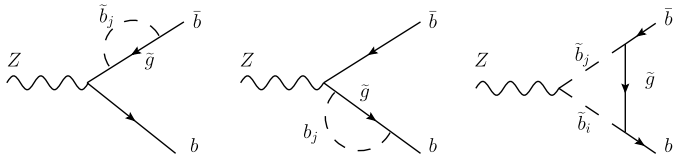

Fig. 1. One-loop Feynman diagrams of gluino correction to $Z \to \bar{b}b$.

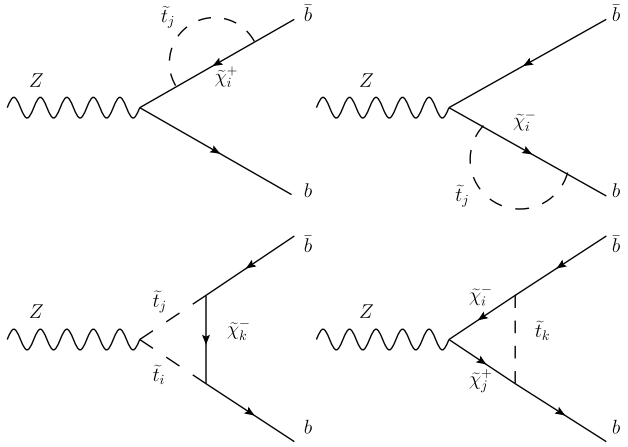

Fig. 2. One-loop Feynman diagrams of chargino correction to $Z \to \bar{b}b$.

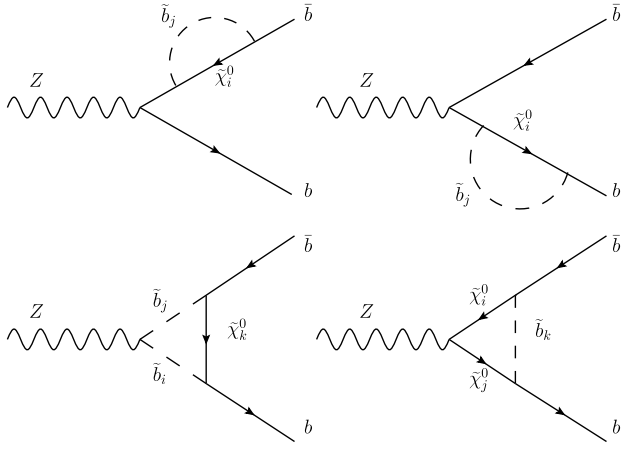

Fig. 3. One-loop Feynman diagrams of neutralino correction to $Z \to \bar{b}b$.

shown in Figs. 1–5. These corrections come from the gluino loops, chargino loops, neutralino loops, charged Higgs loops and neutral Higgs loops.

The one-loop SUSY correction to R_b can be expressed as

$$\delta R_b^{SUSY} \simeq \frac{R_b^{SM}(1-R_b^{SM})}{v_b^2(3-\beta^2)+2a_b^2\beta^2}[v_b(3-\beta^2)\delta v_b + 2a_b\beta^2\delta a_b], \quad (1)$$

where $v_b = 1/2 - 2\sin\theta_w^2/3$ and $a_b = 1/2$ are respectively the vector and axial vector couplings of tree-level $Zb\bar{b}$ interaction, $\beta = \sqrt{1-4m_b^2/m_Z^2}$ is the velocity of bottom quark in $Z \to b\bar{b}$, and δv_b and δa_b are the corresponding corrections defined as [13,16,17]

$$\delta v_b = \frac{\delta g_L^b + \delta g_R^b}{2}, \quad \delta a_b = \frac{\delta g_L^b - \delta g_R^b}{2}. \quad (2)$$

Here δg_λ^b $(\lambda = L, R)$ is give by

$$\delta g_\lambda^b = \Gamma_{f\lambda}(m_Z^2) - g_\lambda^{Zb\bar{b}}\Sigma_{b\lambda}(m_b^2), \quad (3)$$

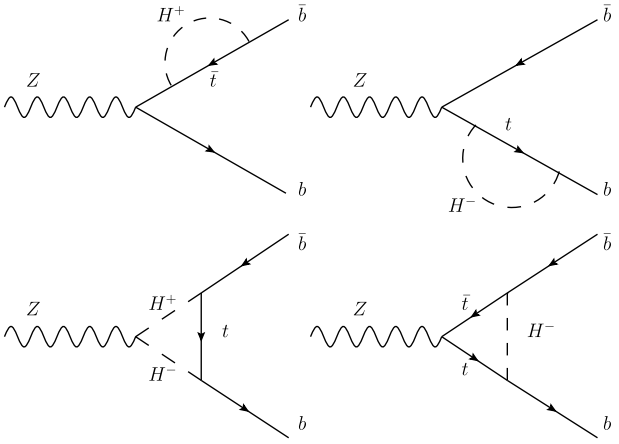

Fig. 4. One-loop Feynman diagrams of charged Higgs correction to $Z \to \bar{b}b$.

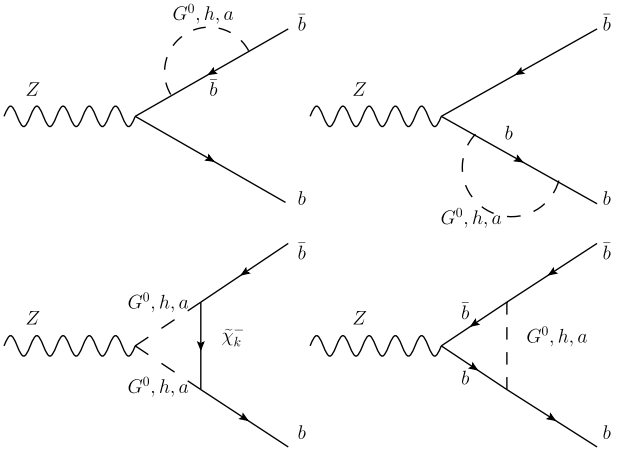

Fig. 5. One-loop Feynman diagrams of neutral Higgs correction to $Z \to \bar{b}b$.

where $\Gamma_{f\lambda}(m_Z^2)$ denotes the vertex loop contributions and $\Sigma_{b\lambda}(m_b^2)$ is the counter term from the bottom quark self-energy. We perform straightforward loop calculations and confirm the expressions in [13]. The results can be expressed as

$$\Sigma_{b_\lambda}(p_b^2) = \frac{C_g}{(4\pi)^2}\left|g_\lambda^{\bar{\psi}_j b\phi_i^*}\right|^2 (B_0 + B_1)(p_b, m_{\phi_i}, m_{\psi_j}), \quad (4)$$

$$\begin{aligned}\Gamma_{b_\lambda}(q^2) = -\frac{C_g}{(4\pi)^2}\Bigg\{ & \left(g_\lambda^{\bar{\psi}_j b\phi_k^*}\right)^* g_\lambda^{\bar{\psi}_i b\phi_k^*}\Big[g_\lambda^{\bar{\psi}_j\psi_i Z} m_{\psi_i} m_{\psi_j} C_0 \\ & + g_{-\lambda}^{\bar{\psi}_j\psi_i Z}\left(-q^2(C_{12}+C_{23}) - 2C_{24} + \frac{1}{2}\right)\Big] \\ & \times (p_{\bar{b}}, p_b, m_{\psi_i}, m_{\phi_k}, m_{\psi_j}) \\ & - \left(g_\lambda^{\bar{\psi}_k b\phi_i^*}\right)^* g_\lambda^{\bar{\psi}_k b\phi_j^*} g^{\phi_i^*\phi_j Z} 2C_{24} \\ & \times (p_{\bar{b}}, p_b, m_{\phi_j}, m_{\psi_k}, m_{\phi_i})\Bigg\}, \end{aligned} \quad (5)$$

where $C_g = 4/3$ for the gluino loops and $C_g = 1$ for other loops, and B_0, B_1 and C_{12}, C_{23}, C_{24} are Passarino–Veltman functions [18]. The notation (ϕ, ψ) represents $(\tilde{b}, \tilde{g})$ for gluino loops, $(\tilde{t}, \tilde{\chi}^-)$ for chargino loops, $(\tilde{b}, \tilde{\chi}^0)$ for neutralino loops, (H^-, t) for charged Higgs loops and $(h/a/G^0, b)$ for neutral Higgs loops.

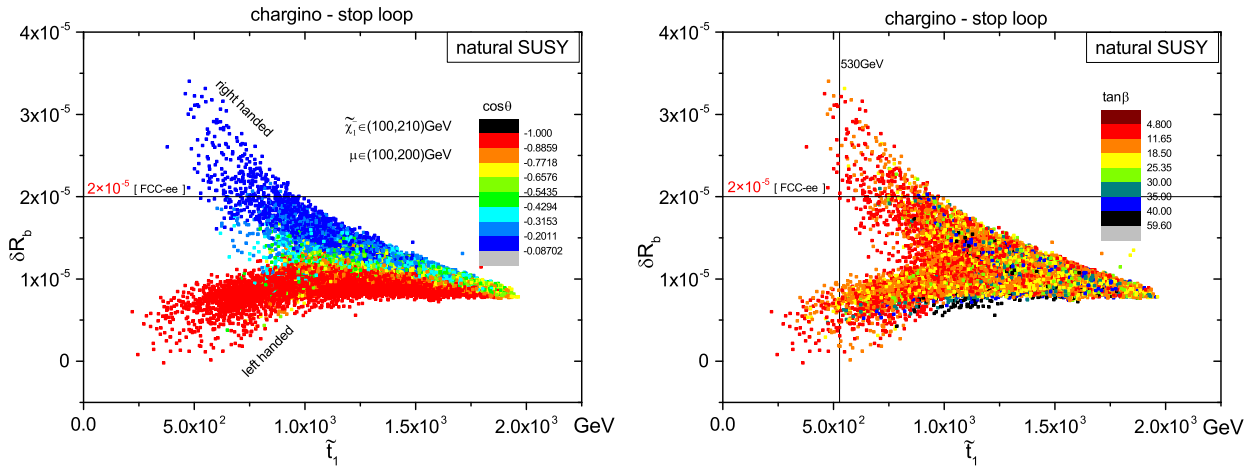

Fig. 6. The scatter plots of the surviving samples of natural SUSY, showing the chargino one-loop effects in R_b.

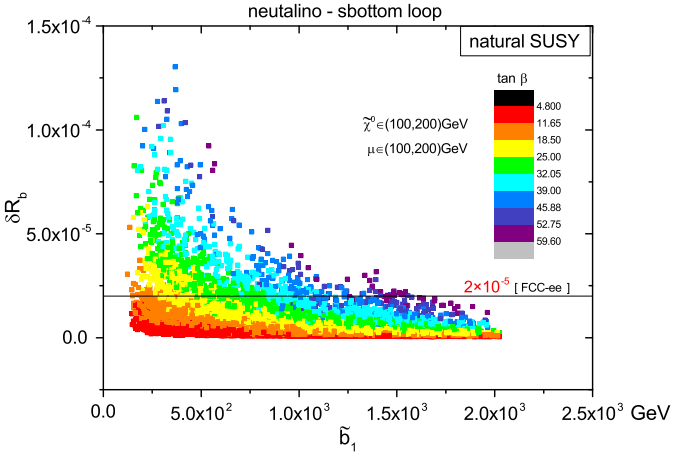

Fig. 7. Same as Fig. 6, but showing the neutralino loop effects.

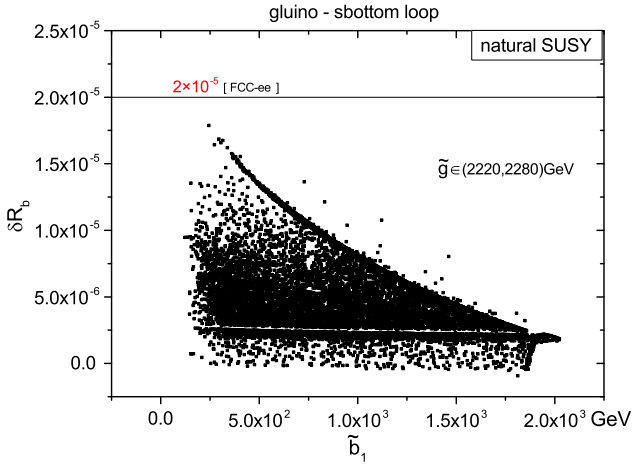

Fig. 8. Same as Fig. 6, but showing the gluino loop effects.

In addition to R_b, we also show the SUSY effects in the forward-backward asymmetry A_{FB}^b in the decay $Z \to \bar{b}b$:

$$\delta A_{FB}^b|_{SUSY} \simeq A_{FB}^b|_{SM}\left(\frac{v_b\delta v_b + a_b\delta a_b}{a_b v_b} - 2\frac{v_b(3-\beta^2)\delta v_b + 2a_b\beta^2\delta a_b}{v_b^2(3-\beta^2)+2a_b^2\beta^2}\right). \quad (6)$$

Its experimental value is 0.0992 ± 0.0016 from the LEP experiment [5] while its SM prediction is 0.1032 ± 0.0004 [19]. In the future Z-factories, this forward-backward asymmetry will be measured together with R_b, both of which will jointly allow for a revelation of SUSY effects.

3. Numerical calculations and results

3.1. SUSY parameter space

To clarify our numerical calculations we consider the general MSSM and the natural-SUSY scenario [20]. From the natural-SUSY results (the natural-SUSY parameter space is much smaller than the general MSSM), we can acquire the more detailed characters of each kind of loops, while from the general MSSM results we can obtain the more general size of SUSY loop effects.

For the natural-SUSY scenario, since in this scenario only the higgsino masses and the third-generation squark masses are assumed to be light, while other sparticles are assumed to be rather heavy and thus their effects in low energy observables are decoupled, in our scan we fix the soft-breaking mass parameters in the first two generation squark sector and the slepton sector at 5 TeV, and assume $A_t = A_b$. For the electroweak gaugino masses, inspired by the grand unification relation, we take $M_1 : M_2 = 1 : 2$ and fix M_2 at 2 TeV. The gluino mass is fixed at 2 TeV since it is supposed to be not too far above TeV scale in natural-SUSY. Other parameters vary as follows

$$1 < \tan\beta < 60,\ 100\ \text{GeV} < \mu < 200\ \text{GeV},\ |A_t| < 3\ \text{TeV},$$
$$100\ \text{GeV} < m_{Q_3}, m_{U_3}, m_{D_3} < 2\ \text{TeV}. \quad (7)$$

For the general MSSM, assuming $A_t = A_b$ and $M_1 : M_2 : M_3 = 1 : 2 : 6$, we scan over the following parameter space

$$1 < \tan\beta < 60,\ 100\ \text{GeV} < \mu < 1000\ \text{GeV},\ |A_t| < 3\ \text{TeV},$$
$$100\ \text{GeV} < m_{Q_3}, m_{U_3}, m_{D_3} < 2\ \text{TeV},\ 100\ \text{GeV} < M_2 < 20000\ \text{GeV}. \quad (8)$$

In our scan we consider the following experimental constraints:

(1) The constraints on the Higgs sector from the LEP, Tevatron and LHC experiments. We use the package HiggsBounds-4.0.0 [21] to implement these constraints.
(2) The experimental constraints in B-physics. We require SUSY to satisfy various B-physics bounds at 2σ level with SUSY FLAVOR v2.0 [22], which includes $B \to X_s\gamma$, $B_s \to \mu^+\mu^-$, $B^+ \to \tau^+\nu$ and so on [23].

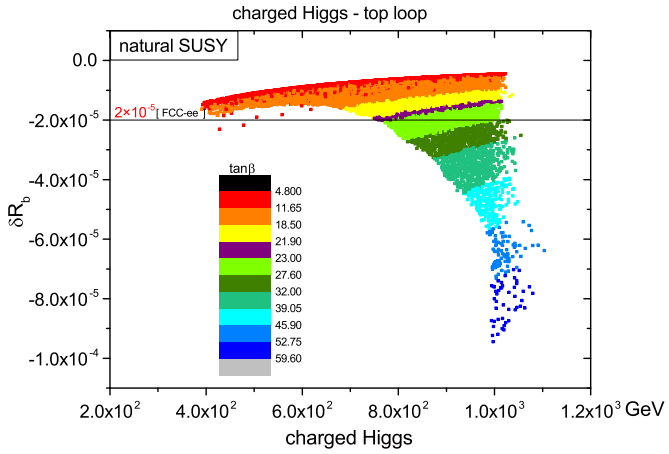

Fig. 9. Same as Fig. 6, but showing the charged Higgs loop effects.

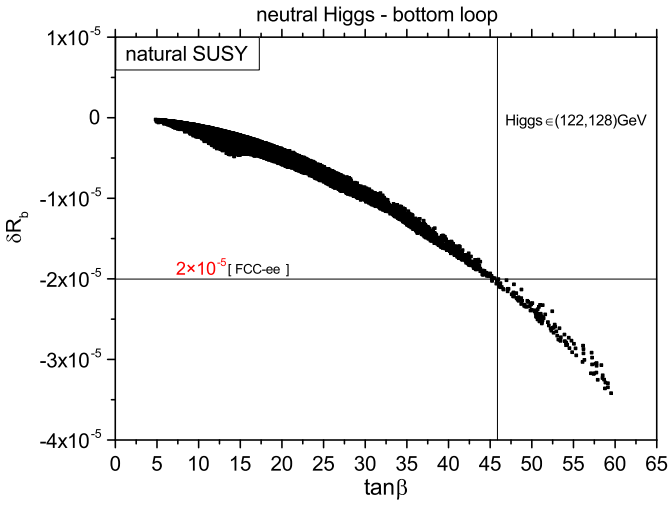

Fig. 10. Same as Fig. 6, but showing the neutral Higgs loop effects.

(3) The measurements of the precision electroweak observables. The SUSY predictions of ρ_l, $\sin^2\theta^l_{eff}$ and m_W are required to be within the 2σ ranges of the experimental values [5].

(4) The dark matter constraints. We require the thermal relic density of the neutralino dark matter to be below the 2σ upper limit of the Planck value [24] and require the dark matter-nucleon spin-independent scattering scross section σ_r^{SI} to satisfy the 95% C.L. limits of LUX [25]. We also consider the limits of spin-dependent dark matter-nucleon cross section σ_r^{SD} from the XENON100 experiment [26]. The relic density, σ_r^{SI} and σ_r^{SD} are calculated with the code MicrOmega v2.4 [27].

About the mass bounds from the LHC direct searches, in natural SUSY the higgsinos have very weak bounds because their pair productions only give missing energy and are rather difficult to detect (a mono-jet or mono-Z is needed in detection) [28], while for the stops the right-handed one is weakly bounded (its mass can be as light as 210 GeV for higgsinos heavier than 190 GeV) [29]. When we display the numerical results, we will not show a sharp LHC bound on stop or higgsino mass (we only consider the LEP bounds on stop and higgsinos). For each surviving sample we calculate the correction to R_b and display the numerical results in the proceeding section.

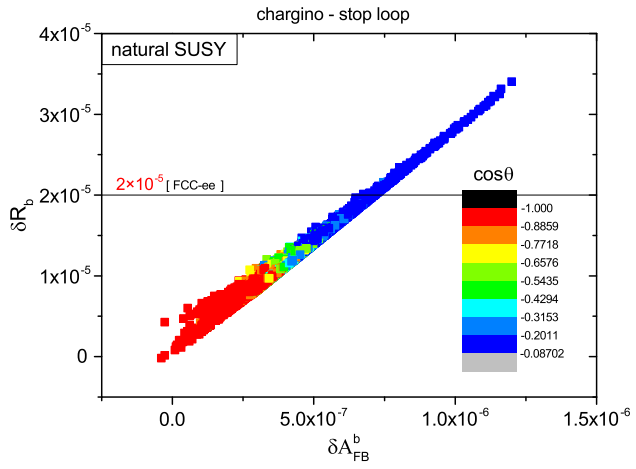

Fig. 11. Same as Fig. 6, but showing δR_b versus δA^b_{FB}.

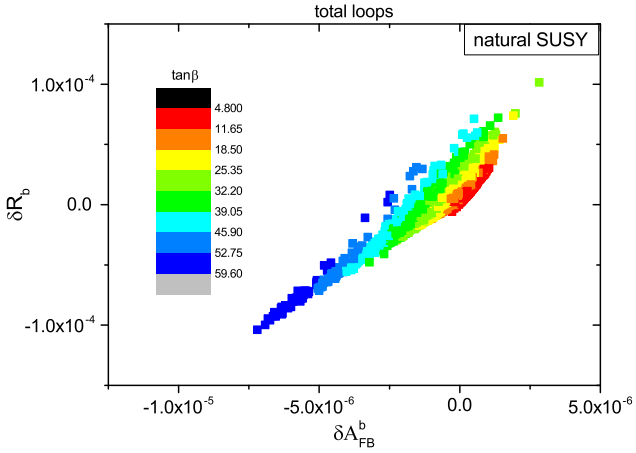

Fig. 12. Same as Fig. 11, but for the combined loop effects.

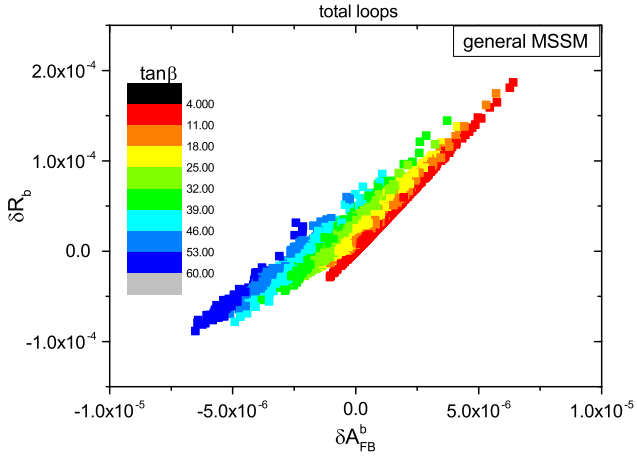

Fig. 13. Same as Fig. 12, but for the general MSSM.

3.2. Numerical results of R_b and A^b_{FB}

The results for natural-SUSY and the general MSSM are displayed in Figs. 6–12 and Figs. 13–14, respectively. We first show the results of different loops and then show the combined results. Finally we compare the natural-SUSY results with the general MSSM results.

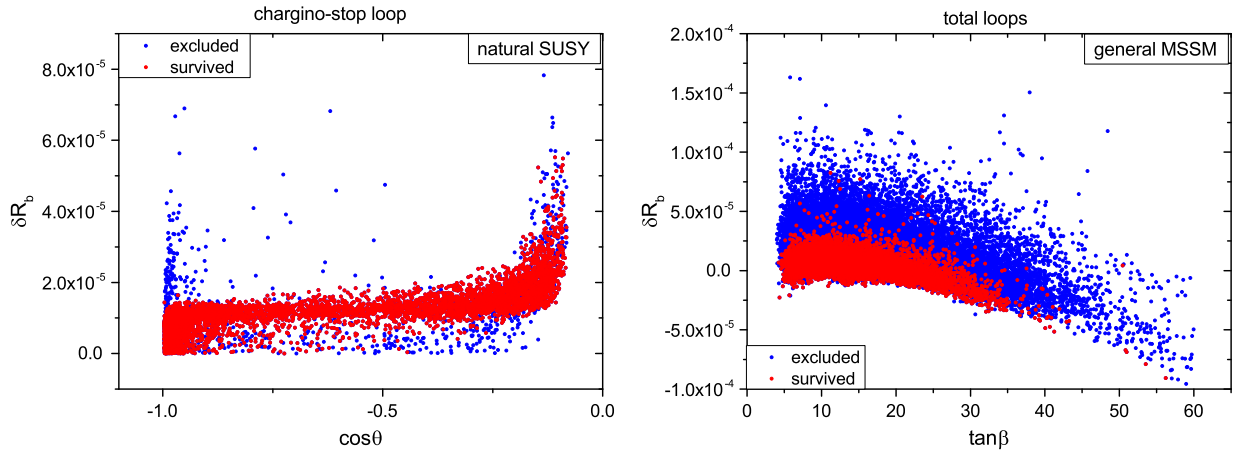

Fig. 14. The plots of survived samples, showing the most sensitive restrictions in two scenarios. The left panel is for natural SUSY, where the samples with and without B-physics constraints are displayed (other constraints are satisfied). The right panel is for the general MSSM, where the samples with and without the dark matter-nucleon spin-independent scattering limits are displayed (other constraints are satisfied).

About the future precision of R_b measurement, the CEPC would produce 10^{10} Z-bosons and probably measure R_b with an uncertainty of 1.7×10^{-4} [8,11], while the FCC-ee could produce 10^{12} Z-bosons and give a much better R_b measurement at 10^{-5} level [9]. In our figures, for illustration, we mark an uncertainty of 2×10^{-5} [9,11]. The SUSY parameter space giving $\delta R_b^{SUSY} > 2 \times 10^{-5}$ corresponds to the observable region.

Some discussions about the results are in order:

(a) From Fig. 6 we see that the chargino-stop loop effects are sizable only if $\tilde{t}_1$ is dominated by a right-handed stop. For a left-handed stop, its coupling with higgsino and bottom $Y_b = gm_b/(\sqrt{2}m_W \cos\beta)$ is suppressed (the lightest chargino $\tilde{\chi}_1^{\pm}$ is dominated by higgsino component since the higgsino mass μ is much smaller than the gaugino masses M_1 and M_2 in natural SUSY). Only for a very large $\tan\beta$ can the coupling Y_b be comparable to the corresponding right-handed stop coupling $Y_t = gm_t/(\sqrt{2}m_W \sin\beta)$. Our numerical results shows that $\tan\beta$ is smaller than 35 (so that $Y_b/Y_t < 1$) for $\tilde{t}_1$ below 530 GeV (when $\tan\beta$ is larger, $\tilde{t}_1$ must be heavier to satisfy the experimental constraints). Note that, as commented in the preceding section, so far the right-handed stop mass in natural SUSY is weakly bounded by LHC experiments (its mass can be as light as 210 GeV for higgsinos heavier than 190 GeV) [29].

(b) As shown in Fig. 8, the gluino-sbottom loop effects are very small due to the heaviness of gluino. The loop effects of the neutralinos, charged and neutral Higgs bosons, as shown in Figs. 7, 9 and 10, are sensitive to $\tan\beta$ and can be sizable for a large value of $\tan\beta$. Our numerical results show that the neutralino loop can push the $\tilde{b}_1$ mass to 850 GeV when $\tan\beta$ is around 32. If the $\tan\beta$ is about 23, through the charged Higgs loop, $\tilde{H}^+$ mass less than 770 GeV is excluded. The neutral Higgs loops impose an upper bound of 46 on the value of $\tan\beta$.

(c) From Figs. 11, 12 and 13 we see that the SUSY effects in R_b and A_{FB}^b are correlated, as expected. Both observables can jointly probe the SUSY effects. While the chargino loop effects always enhance both quantities, the combined total effects of all loops can either enhance or reduce them. We also find that in the general MSSM without special naturalness requirement, both R_b and A_{FB}^b are allowed to vary in a larger region than in natural SUSY, especially when $\tan\beta$ is small.

(d) From Figs. 6–13 we see that in some currently allowed parameter space, the effects of natural SUSY may be accessible in the future R_b measurement. If it can be measured with an uncertainty of 2×10^{-5}, a large part of SUSY parameter space can be covered.

(e) We found that for natural SUSY the most stringent limits are from B-physics, while for the general MSSM the most stringent limits are from the dark matter-nucleon spin-independent scattering limits. The results are shown in Fig. 14. Other constraints, such as the dark matter-nucleon spin-dependent scattering cross section, are also making impacts but not as stringent as these two.

4. Conclusion

We revisited the SUSY effects in R_b under current experimental constraints including the LHC Higgs data, the B-physics measurements, the dark matter relic density and direct detection limits, as well as the precision electroweak data. We scanned over the SUSY parameter space and in the allowed parameter space we displayed the SUSY effects in R_b. We found that although the SUSY parameter space has been severely restrained by current experimental data, SUSY can still alter R_b with a magnitude sizable enough to be observed at future Z-factories (ILC, CEPC, FCC-ee). Assuming a precise measurement $\delta R_b = 2.0 \times 10^{-5}$ at FCC-ee, we can probe the right-handed stop to 530 GeV through the chargino-stop loops, probe the sbottom to 850 GeV through the neutralino-sbottom loops and the charged Higgs to 770 GeV through the Higgs-top quark loops for a large $\tan\beta$. The full one-loop SUSY correction to R_b can reach 1×10^{-4} in natural SUSY and 2×10^{-4} in the general MSSM.

Acknowledgements

We would like to thank Junjie Cao, Lei Wu, Yang Zhang, Mengchao Zhang for useful discussions. This work has been supported in part by the National Natural Science Foundation of China under grant Nos. 11275245 and 11135003, and by the CAS Center for Excellence in Particle Physics (CCEPP).

References

[1] S. Chatrchyan, et al., CMS Collaboration, Phys. Lett. B 716 (2012) 30, arXiv:1207.7235 [hep-ex].
[2] G. Aad, et al., ATLAS Collaboration, Phys. Lett. B 716 (2012) 1, arXiv:1207.7214 [hep-ex].

[3] See, e.g. J. Cao, et al., J. High Energy Phys. 1203 (2012) 086, arXiv:1202.5821 [hep-ph];
J. Cao, et al., J. High Energy Phys. 1210 (2012) 079, arXiv:1207.3698 [hep-ph].
[4] A. Djouadi, et al., Nucl. Phys. B 349 (1991) 48.
[5] S. Schael, et al., ALEPH and DELPHI and L3 and OPAL and SLD and LEP Electroweak Working Group and SLD Electroweak Group and SLD Heavy Flavour Group Collaborations, Phys. Rep. 427 (2006) 257, arXiv:hep-ex/0509008.
[6] A. Freitas, J. High Energy Phys. 1404 (2014) 070, arXiv:1401.2447 [hep-ph].
[7] H. Baer, et al., The International Linear Collider technical design report – volume 2: physics, arXiv:1306.6352.
[8] M. Ahmad, et al., CEPC-SPPC preliminary conceptual design report, volume I: physics and detector, http://cepc.ihep.ac.cn/preCDR/volume.html;
Z. Liang, Z and W physics at CEPC, http://indico.ihep.ac.cn/event/4338/session/2/material/slides/1?contribId=32.
[9] M. Bicer, et al., TLEP Design Study Working Group Collaboration, J. High Energy Phys. 1401 (2014) 164, arXiv:1308.6176 [hep-ex].
[10] J.-P. Ma, C.-H. Chang, Sci. China, Phys. Mech. Astron. 53 (2010) 1947.
[11] J. Fan, M. Reece, L.T. Wang, arXiv:1412.3107 [hep-ph];
S. Gori, J. Gu, L.T. Wang, arXiv:1508.07010 [hep-ph].
[12] M. Boulware, D. Finnell, Phys. Rev. D 44 (1991) 2054.
[13] J. Cao, J.M. Yang, J. High Energy Phys. 0812 (2008) 006, arXiv:0810.0751 [hep-ph].
[14] D. Garcia, R.A. Jimenez, J. Sola, Phys. Lett. B 347 (1995) 321, arXiv:hep-ph/9410311;
D. Garcia, R.A. Jimenez, J. Sola, Phys. Lett. B 347 (1995) 309, arXiv:hep-ph/9410310;
D. Garcia, J. Sola, Phys. Lett. B 357 (1995) 349, arXiv:hep-ph/9505350;
D. Garcia, J. Sola, Phys. Lett. B 354 (1995) 335, arXiv:hep-ph/9502317.
[15] J.D. Wells, C.F. Kolda, G.L. Kane, Phys. Lett. B 338 (1994) 219;
D.M. Pierce, J.A. Bagger, K.T. Matchev, R. Zhang, Nucl. Phys. B 491 (1997) 3;
G. Altarelli, R. Barbieri, F. Caravaglios, Phys. Lett. B 314 (1993) 357;
J.M. Yang, Eur. Phys. J. C 20 (2001) 553;
J. Cao, Z. Xiong, J.M. Yang, Phys. Rev. Lett. 88 (2002) 111802.
[16] M. Bohm, H. Spiesberger, W. Hollik, Fortschr. Phys. 34 (1986) 687.
[17] W. Hollik, Fortschr. Phys. 38 (1990) 165.
[18] G. Passarino, M. Veltman, Nucl. Phys. B 160 (1979) 151.
[19] M. Baak, et al., Gfitter Group Collaboration, Eur. Phys. J. C 74 (2014) 3046, arXiv:1407.3792 [hep-ph].
[20] See, e.g. M. Papucci, J.T. Ruderman, A. Weiler, J. High Energy Phys. 1209 (2012) 035, arXiv:1110.6926 [hep-ph];
L.J. Hall, D. Pinner, J.T. Ruderman, J. High Energy Phys. 1204 (2012) 131, arXiv:1112.2703 [hep-ph];
H. Baer, et al., Phys. Rev. Lett. 109 (2012) 161802;
H. Baer, et al., Phys. Rev. D 87 (2013) 115028.
[21] P. Bechtle, et al., arXiv:1102.1898 [hep-ph];
P. Bechtle, et al., arXiv:0811.4169 [hep-ph].
[22] A. Crivellin, et al., Comput. Phys. Commun. 184 (2013) 1004, arXiv:1203.5023 [hep-ph];
J. Rosiek, Comput. Phys. Commun. 188 (2014) 208, arXiv:1410.0606 [hep-ph];
J. Rosiek, et al., Comput. Phys. Commun. 181 (2010) 2180, arXiv:1003.4260 [hep-ph].
[23] K.A. Olive, et al., Particle Data Group Collaboration, Chin. Phys. C 38 (2014) 090001.
[24] P.A.R. Ade, et al., Planck Collaboration, Astron. Astrophys. 571 (2014) A16, arXiv:1303.5076 [astro-ph.CO].
[25] D.S. Akerib, et al., LUX Collaboration, Phys. Rev. Lett. 112 (2014) 091303, arXiv:1310.8214 [astro-ph.CO].
[26] E. Aprile, et al., XENON100 Collaboration, Phys. Rev. Lett. 111 (2013) 021301, arXiv:1301.6620 [astro-ph.CO].
[27] G. Belanger, et al., Comput. Phys. Commun. 182 (2011) 842, arXiv:1004.1092 [hep-ph].
[28] C. Han, et al., J. High Energy Phys. 1402 (2014) 049, arXiv:1310.4274 [hep-ph];
H. Baer, A. Mustafayev, X. Tata, Phys. Rev. D 89 (2014) 055007, arXiv:1401.1162 [hep-ph];
P. Schwaller, J. Zurita, J. High Energy Phys. 1403 (2014) 060, arXiv:1312.7350 [hep-ph];
A. Arbey, M. Battaglia, F. Mahmoudi, Phys. Rev. D 89 (2014) 077701, arXiv:1311.7641 [hep-ph];
A. Arbey, M. Battaglia, F. Mahmoudi, arXiv:1506.02148 [hep-ph];
M. Low, L.T. Wang, J. High Energy Phys. 1408 (2014) 161, arXiv:1404.0682 [hep-ph].
[29] A. Kobakhidze, et al., arXiv:1511.02371 [hep-ph];
J. Fan, et al., arXiv:1512.05781 [hep-ph];
C. Han, et al., J. High Energy Phys. 1310 (2013) 216, arXiv:1308.5307 [hep-ph];
J. Kawamura, Y. Omura, arXiv:1601.03484 [hep-ph];
M. Drees, J.S. Kim, arXiv:1511.04461 [hep-ph].